Title
Multi-Start Foil Wound Solenoids for Multipole Suppression

Authors
Majernik, N
Suraj, A
Fukasawa, A
et al.

Publication Date
2021

ISBN: 978-3-95450-214-1 ISSN: 2673-5490 doi:10.18429/JACoW-IPAC2021-TUPAB094

MULTI-START FOIL WOUND SOLENOIDS FOR MULTIPOLE SUPPRESSION

N. Majernik*, A. Suraj, A. Fukasawa, J. B. Rosenzweig
UCLA, Los Angeles, CA, USA

Abstract

Solenoids for beam transport are typically wound helically, with each layer of wire being laid down on top of the previous, or as "pancakes" where the wire is wound radially in before crossing-over and winding out. Both of these approaches break rotational symmetry and introduce higher order multipole moments which can be deleterious to beam emittance. For high brightness beams, this can be particularly problematic. To this end, a solenoid employing multi-start foil windings is simulated and compared to conventional choices. With appropriate design, this approach can forbid certain multipoles by symmetry.

INTRODUCTION

It is well known that having *stray* (also called *anomalous*) magnetic fields inside a solenoid can lead to emittance degradation and beam asymmetries [1–3] which can be difficult to correct due to the coupled motion between the two transverse planes arising from the beam's rotation in the solenoid. In an idealized, cylindrically symmetric solenoid, the magnetic fields are exclusively longitudinal and radial but asymmetries or misalignments can introduce these problematic transverse fields [4, 5]. The most basic winding approach, *helical winding*, involves winding sequential turns longitudinally along the length of the solenoid, then winding on top of this layer and in the other direction, and repeating this process. This approach may sometimes be sufficient but the need to return current from the innermost layer results in severe symmetry breaking. Therefore, high precision, real-world beamline solenoids often are constructed using *pancake windings* [4, 6, 7]: wire is wound radially inward in layers, then "crosses over" longitudinally by one layer thickness, before winding our radially again (see Fig. 1). This pair of layers constitutes a single pancake and several pancakes can be stacked together longitudinally to fill the length of the solenoid. However, this crossover section still breaks the symmetry of the windings and introduces multipole components. Certain design choices like the angular extent of the crossover and the orientation of adjacent pancakes relative to each other can help reduce the emittance growth but the multipoles are an intrinsic feature of pancake windings.

In this work we present a concept for a multi-start foil wound solenoid. Such a solenoid consists of multiple foils, interspersed with insulating layers, wound onto a central, conducting mandrel. Current is coupled radially into the mandrel, longitudinally along the mandrel, then in spirals out along the foils (see Figs. 2 and 3). By selecting an appropriate number of foils, different multipoles can be forbidden by symmetry [8]. Unlike intrinsically asymmetric windings, this approach can suppress select multipoles up to the level of manufacturing tolerances, offering a much lower floor on the transverse fields. In this work, a particular implementation of a foil wound solenoid is compared computationally with pancake wound solenoids of equal integrated solenoidal field. Other practical considerations for the implementation of such a solenoid, including thermal effects and fabrication, are also discussed.

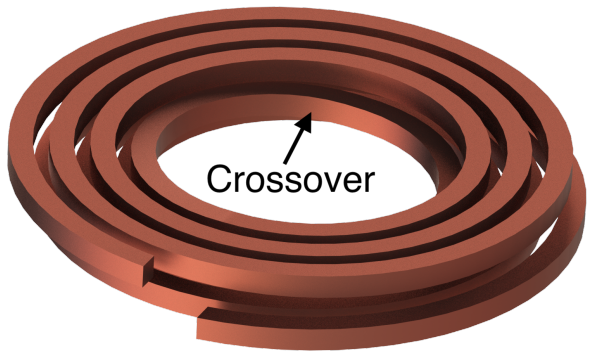

Figure 1: Schematic of a single pancake with crossover called out. Wire spacing is greatly exaggerated for clarity.

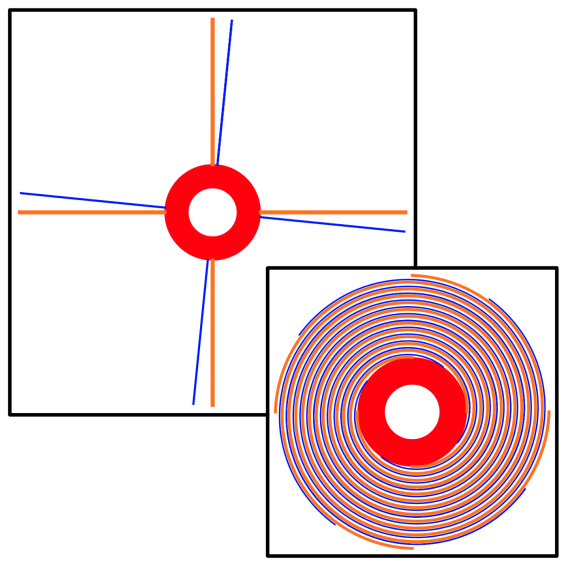

Figure 2: End view schematic of a 4-start foil winding. Red – conducting mandrel, Orange – conducting foil, Blue – insulating layer. (Top left) Foils and insulators connected to mandrel, before winding. (Bottom right) Foils and insulators have been wound onto the mandrel.

* NMajernik@g.ucla.edu

ISBN: 978-3-95450-214-1 ISSN: 2673-5490 doi:10.18429/JACoW-IPAC2021-TUPAB094

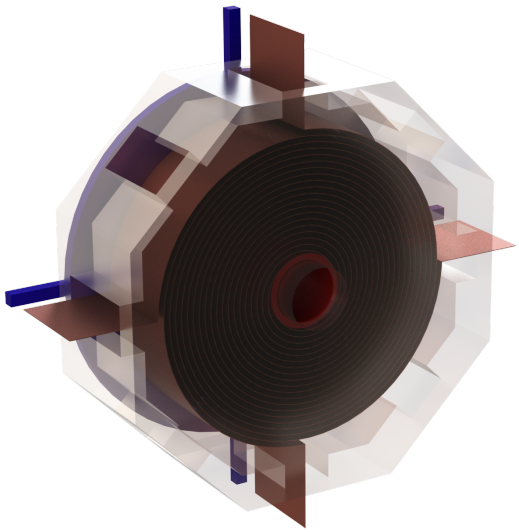

Figure 3: Render of the foil wound model simulated shown with 10 turns rather than the full 100 turns and with the insulating layers omitted; in reality the coil will be tightly wound with no air gaps. The semi-transparent octagonal yoke is the same for all simulation cases. Red – conducting mandrel, Copper – conducting foil, Blue – radial current feed.

SIMULATIONS

For these simulations the solenoid under consideration has a coil length of 80 mm, an inner radius of 30 mm, an outer radius of 130 mm, and achieves a peak field of 0.13 T (integrated field = 0.011 T-m). All simulations will use the same, octagonal yoke (Fig. 3) simulated as 20 mm thick 1006 low carbon steel. Four different scenarios will be presented:

- **Ideal** – A revolved rectangle of uniform current density totalling 8,800 amp-turns.
- **Straight crossover** – Four pancakes, wound with 10 mm square cross section wire, simulated as a filament. Each longitudinal layer has 10 turns (20 per pancake). The crossover is 90° (See [4] for additional details on this convention). Each pancake has the same orientation.
- **Alternating crossover** – Four of the same pancakes with every other pancake rotated 180° about the beam axis.
- **Foil** – 4-start foil winding, 100 turns per foil. The radial current feed is immediately outside the upstream end of the yoke.

The presented results are from simulations performed using the magnetostatics code *RADIA* [9]. *RADIA* employs the boundary integral method of field computation which, in contrast with finite element analysis (FEA), does not require the vacuum to be meshed. This helps reduce the computational demands of these high precision simulations. However, since no symmetry approximations may be made, the whole model must be simulated which is still computationally expensive.

Current Distribution

RADIA must be provided with the current distribution and cannot calculate it from a description of the conductor geometry. For the foil case it was assumed that: the radial current feed was uniform; the longitudinal current feed was linearly diminishing along the length of the mandrel; and the foil current was uniformly distributed within each foil. A current distribution with these assumptions was discretized and simulated as thin current filaments.

The finite element analysis code CST [10] was given a full description of the conductor geometry and fully simulated the resulting current distribution. This current distribution was used in its FEA magnetostatics solver and it showed good agreement with the magnetic fields from *RADIA* arising from the approximated current distribution.

Multipole Decomposition

Many sources offer detailed descriptions of multipole decompositions (*e.g.* [8, 11]) but such a discussion is beyond the scope of this work. Instead we only assert the convention used:

$$B_\phi(\phi) = a_0 + \sum_{k=1}^{\infty} (a_k \cos k\phi + b_k \sin k\phi). \qquad (1)$$

B_ϕ is the azimuthal magnetic field described on some circle with radius r. The resulting coefficients give the normal and skew multipole component strengths according to $a_k r^{-k+1}$ and $b_k r^{-k+1}$ respectively. $k = 1$ corresponds to the dipole component, $k = 2$ to the quadupole, and so on. These values can be calculated at every longitudinal position.

Results

A summary of the results is shown by Fig. 4 which shows the on-axis field as well as the dipole, quadrupole, and sextupole components. The longitudinal fields are visually indistinguishable between the four cases. The dipole fields are the greatest for the straight crossover case; by alternating the orientation of the pancakes, the contributions from adjacent pancakes are mitigated. The ideal and foil wound cases are identically zero. For the quadrupole field, the straight and alternating crossover configurations are nearly the same; the interaction with the iron yoke leads to a slight deviation between the two cases. For the quadrupole and sextupole moments, the ideal and foil cases both are still zero. These results support the claim that multi-start foil windings can suppress multipoles by symmetry. Designs with more foils could suppress even higher order harmonics but a 4-start design was selected to simplify fabrication.

ISBN: 978-3-95450-214-1 ISSN: 2673-5490 doi:10.18429/JACoW-IPAC2021-TUPAB094

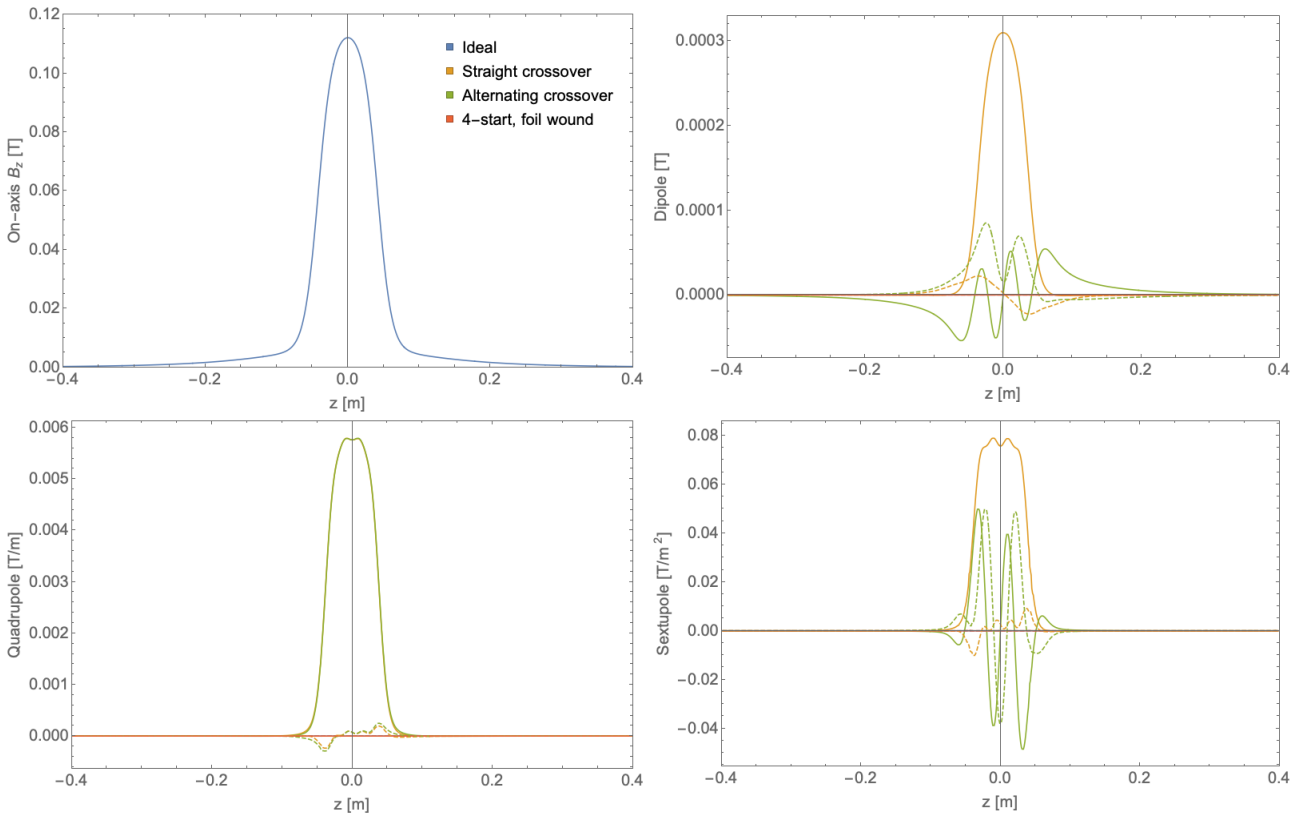

Figure 4: Plots showing fields along the length of the proposed solenoid with different winding strategies. Solid lines are the "normal" component and dashed lines are the "skew" component. (Top left) On axis solenoid field; fields between different cases are visually indistinguishable. (Top right) Dipole component. Both the ideal and foil wound cases are zero. (Bottom left) Quadrupole component. The straight and alternating crossover cases approximately overlap with deviations arising from their interaction with the iron yoke. Both the ideal and foil wound cases are zero. (Bottom right) Sextupole component. Both the ideal and foil wound cases are zero.

DISCUSSION AND FUTURE WORK

One issue that a foil wound solenoid faces is that of cooling. Often, solenoids are wound with hollow wire and water cooled but this is not an option when using foil. Instead, such solenoids must be cooled by conduction through the inner mandrel and outer surface of the foils. Thermal calculations for the solenoid presented here, assuming thin insulating layers of polyimide (often referred to as *Kapton*, a registered trademark of DuPont), indicate a maximum local temperature rise of only a few degrees. However, for solenoids requiring appreciably higher fields and current densities, foil winding may not be a viable option.

The first embodiment of this design will be for use with a cryogenic, high gradient photocathode testbed at UCLA [12, 13] which is anticipated to produce extremely low emittance beams. Beam dynamics simulations will be conducted to ensure that the non-suppressed multipoles do not excessively degrade the beam's emittance and mechanical tolerances for fabrication will be established. Plans for in-house winding of such a solenoid are in progress. Field characterization might be done using the 3D Hall probe gantry built for characterizing the magnets of [14] and also with a new, rotating coil setup. In the future, this concept may be extended for use at cryogenic temperatures for other applications requiring extremely bright beams [15, 16].

ACKNOWLEDGMENTS

This work was supported by the National Science Foundation through the Center for Bright Beams, Grant No. PHY-1549132 and the US Dept. of Energy, Division of High Energy Physics, under contract DE-SC0020409.

REFERENCES

[1] D. H. Dowell, "Sources of emittance in rf photocathode injectors: Intrinsic emittance, space charge forces due to non-uniformities, rf and solenoid effects", 2016. arXiv:1610.01242

[2] L. Zheng *et al.*, "Overestimation of thermal emittance in solenoid scans due to coupled transverse motion", *Phys. Rev. Accel. Beams*, vol. 21, no. 12, p. 122803, 2018. doi:10.1103/physrevaccelbeams.21.122803

[3] Q. Zhao *et al.*, "Beam asymmetry studies with quadrupole field errors in the PITZ gun section", in *Proc. FEL'17*, Santa Fe, NM, USA, Aug. 2017, pp. 440-443. doi:10.18429/JACoW-FEL2017-WEP010

ISBN: 978-3-95450-214-1 ISSN: 2673-5490 doi:10.18429/JACoW-IPAC2021-TUPAB094

[4] X. Gu, M. Okamura, A. Pikin, W. Fischer, and Y. Luo, "The effects of realistic pancake solenoids on particle transport", *Nucl. Instrum. Methods Phys. Res., Sect. A*, vol. 637, no. 1, pp. 190–199, 2011. doi:10.2172/1007888

[5] J. Schmerge, "LCLS gun solenoid design considerations", SLAC National Accelerator Lab, Menlo Park, CA, USA, Rep. LCLS-TN-05-14, 2005.

[6] G. D'Auria *et al.*, "The new photoinjector for the FERMI project", in *Proc. 22nd Particle Accelerator Conference (PAC'07)*, Albuquerque, NM, USA, Jun. 2007, paper TUPMN028, pp. 974-976.

[7] W. Fischer, Z. Altinbas, M. Anerella, and E. Beebe, "Construction progress of the RHIC electron lenses", Brookhaven National Laboratory, Upton, NY, USA, Rep. BNL-96671-2012-CP, 2012.

[8] J. T. Tanabe, *Iron dominated electromagnets: design, fabrication, assembly and measurements*. Hackensack, NJ, USA: World Scientific Publishing Company, 2005.

[9] O. Chubar, P. Elleaume, and J. Chavanne, "A three-dimensional magnetostatics computer code for insertion devices", *J. Synchrotron Radiat.*, vol. 5, no. 3, pp. 481–484, 1998. doi:10.1107/s0909049597013502

[10] CST studio suite – electromagnetic field simulation software, https://www.3ds.com/products-services/simulia/products/cst-studio-suite/.

[11] A. K. Jain, "Basic theory of magnets", *CAS - CERN Accelerator School : Measurement and Alignment of Accelerator and Detector Magnets*, pp. 1–6, 1998. doi:10.5170/CERN-1998-005.1

[12] G. Lawler *et al.*, "UCLA facility for development and testing of novel photoinjectors", *Bulletin of the American Physical Society*, vol. 65, no. 2, 2020.

[13] G. E. Lawler, A. Fukasawa, N. Majernik, M. Yadav, A. Suraj, and J. B. Rosenzweig, "Rf testbed for cryogenic photoemission studies", presented at the 12th Int. Particle Accelerator Conf. (IPAC'21), Campinas, Brazil, May 2021, paper WEPAB096, this conference.

[14] N. Majernik *et al.*, "Optimization of low aspect ratio, iron dominated dipole magnets", *Phys. Rev. Accel. Beams*, vol. 22, no. 3, p. 032401, 2019. doi:10.1103/physrevaccelbeams.22.032401

[15] J. B. Rosenzweig *et al.*, "An ultra-compact x-ray free-electron laser", *New J. Phys.*, vol. 22, no. 9, p. 093067, 2020. doi:10.1088/1367-2630/abb16c

[16] R. R. Robles *et al*, "Versatile, high brightness, cryogenic photoinjector electron source", *Phys. Rev. Accel. Beams*, vol. 24, no. 6, p. 063401, 2021. doi:10.1103/physrevaccelbeams.24.063401